Journal of Chromatography A, 1230 (2012) 54–60

Contents lists available at SciVerse ScienceDirect

Journal of Chromatography A

journal homepage: www.elsevier.com/locate/chroma

Preparation and characterization of methacrylate-based monolith for capillary hydrophilic interaction chromatography

Ming-Luan Chen[a], Li-Man Li[a], Bi-Feng Yuan[a], Qiao Ma[b], Yu-Qi Feng[a,*]

[a] Key Laboratory of Anal. Chem. for Biology and Medicine (Ministry of Education), Department of Chemistry, Wuhan University, Wuhan 430072, China
[b] Focused Photonics (Hangzhou), Inc., Hangzhou 310052, China

ARTICLE INFO

Article history:
Received 13 November 2011
Received in revised form 18 January 2012
Accepted 23 January 2012
Available online 30 January 2012

Keywords:
Capillary liquid chromatography
Organic polymer monolith
Hydrophilic liquid chromatography
Poly(methacrylic acid-*co*-ethylene glycol dimethacrylate) monolith

ABSTRACT

In current study, poly(methacrylic acid-*co*-ethylene glycol dimethacrylate) (MAA-*co*-EDMA) monolith was successfully prepared for capillary hydrophilic liquid chromatography (*c*HILIC). The polymerization was optimized by changing the ratio of MAA to EDMA, the type and amount of porogen. The characterization indicated that "hydrophilic" monolithic column possessed homogeneous column bed, good permeability and narrow pore size distribution. Under HILIC mode, the "hydrophilic" monolith prepared with PEG and DMSO showed stronger hydrophilicity than the "hydrophobic" monolith prepared with dodecanol and toluene. Finally, the "hydrophilic" monolith was applied in the separation of tryptic digests of bovine serum albumin (BSA) with *c*HILIC-ESI-qTOF–MS system. Our results revealed that 49 peptides were identified with 50% sequence coverage under HILIC mode, which was much better than the peptides identified using particulate-packed commercial column with RPLC-ESI-qTOF–MS system or "hydrophobic" monolith with *c*HILIC-ESI-qTOF–MS system. Taken together, the "hydrophilic" monolithic column prepared in current study, demonstrated the excellent chromatographic performance on the separation of complex samples, which offers the potential application of the monolith on proteomics study.

1. Introduction

Since hydrophilic interaction chromatography (HILIC) was introduced and investigated systematically by Alpert in 1990 [1], it has become a useful complementary technique to reversed-phase chromatography (RPLC) [2–4]. Up to date, based on hydrophilic monolithic materials, hydrophilic capillary electrochromatography (HI-CEC) and capillary HILIC (*c*HILIC) have been successfully applied in the separation of various types of analytes, including proteins [5,6], peptides [7,8], DNA and nucleotides [5,9–11], carbohydrates [12,13], and some small polar molecules [11,14,15]. More recently, several peptides such as dipeptides, bioactive peptides, and protein digests were successfully separated using HILIC with good resolution, indicating the promising role of HILIC in proteomics study [7,16–18].

Since porous polymer-based monoliths were initially introduced for capillary liquid chromatography (*c*LC) [3,19], the monolithic materials were intensively used as stationary phase for *c*LC. Compared to silica-based monolith with hydrophilic skeleton, polymer-based monolith employs hydrophilic and/or ionic monomers to obtain sufficient hydrophilicity. In this respect, a variety of polymer-based monoliths with hydroxyl [20,21], amino [22–25], amide [26,27], cyano [28], sulfonic [29–31], carboxylic groups [32,33] have been prepared with high column efficiency for *c*LC [7,34–36]. However, few study on the influence of porogen systems on the surface polarity of monolith has been reported [21].

Poly(ethylene glycol) (PEG), firstly applied as porogen by Novoty's group [37], can induce the formation of desired porous structure and homogeneous column bed. PEG has hydrophilic heads comprised of hydroxyl groups ($HO–(CH_2–CH_2–O)_n–H$), which can provide good water-solubility [38,39]. Courtois et al. also demonstrated that PEG can form a "water-friendly" surface on through-pores [38]. According to our previous study, the microglobules and pore size distribution of monolith can be adjusted by changing the amount and molecular weight of PEG [37,40]. Under optimized conditions, large through-pores, narrow pore size distributions and homogeneous column bed can be obtained for the monolith prepared with PEG.

In our current study, poly(methacrylic acid-*co*-ethylene glycol dimethacrylate) monolith (MAA-*co*-EDMA) was prepared inside a 100 μm *i.d.* capillary using hydrophilic porogen system—PEG and dimethyl sulfoxide (DMSO), or hydrophobic porogenic solvents—dodecanol and toluene. The polymerization conditions were optimized by changing the ratio of MAA to EDMA, the types and amount of porogens. The pore structure and hydrophilicity of monolith and the number of carboxylic acid group on the monolithic surface were compared between "hydrophilic" and "hydrophobic" monolithic columns. The chromatographic

* Corresponding author. Tel.: +86 27 68755595; fax: +86 27 68755595.
E-mail address: yqfeng@whu.edu.cn (Y.-Q. Feng).

0021-9673/$ – see front matter © 2012 Elsevier B.V. All rights reserved.
doi:10.1016/j.chroma.2012.01.065

Table 1
The ratio of MAA to EDMA used for the preparation of monoliths and the permeability (K) measured for each monolith.[a]

Monolith	MAA (%, $w/w_{total\ monomers}$)	EDMA (%, $w/w_{total\ monomers}$)	K ($\times 10^{-13}$ m^2)
Column 1	5.00	95.0	4.50
Column 2	6.50	93.5	10.20
Column 3	8.00	92.0	19.50
Column 4	10.00	90.0	23.00
Column 5	12.50	87.5	29.30

[a] The ratio of monomers (MAA and EDMA), PEG-6000 and DMSO is 1/1/3 (w/w/w).

Table 2
Permeability (K) and specific surface areas of the monoliths prepared with PEG of different molecular weight.[a]

Monolith	PEG M.W.	K ($\times 10^{-13}$ m^2)	Specific surface area (m^2/g)
Column 6	2000	3.38	169
Column 7	4000	16.50	142
Column 8	6000	23.60	100
Column 9	10,000	36.90	71

[a] The ratio of monomers (MAA and EDMA), PEG-6000 and DMSO is 1/1/3 (w/w/w). The percent of MAA and EDMA ($w/w_{total\ monomers}$) is 8% and 92%, respectively.

performance of the resulting monolithic column was evaluated by different kinds of compounds, including nucleosides, anilines and benzoic acids in HILIC mode. Finally, the "hydrophilic" monolithic column was applied in the separation of tryptic digests of bovine serum albumin (BSA) using *c*HILIC-ESI-qTOF–MS system.

2. Materials and methods

2.1. Chemicals and buffers

MAA (98 wt% pure, containing 250 ppm monomethyl ether hydroquinone (MEHQ) as inhibitor) and EDMA (98 wt% pure, containing 90–110 ppm MEHQ as inhibitor) were purchased from Acros (New Jersey, USA). Azobisisobutyronitrile (AIBN), PEG with molecular weight from 2000 to 10,000, and DMSO were all purchased from Shanghai Chemical Reagent Corporation (Shanghai, China). 3-(Triethoxysilyl) propyl methacrylate was purchased from Wuhan University Silicone New Material (Wuhan, China). HPLC-grade methanol and acetonitrile (ACN) were obtained from TEDIA Company (Ohio, USA). The water used throughout all experiments was purified using a Milli-Q water purification system (Millipore, Bradford, USA). The fused-silica capillaries were purchased from Yongnian Optic Fiber Plant (Hebei, China).

Thiourea, benzene, toluene, ethylbenzene, propylbenzene, anilines, benzoic acids, acrylamide, ammonium acetate were of analytical grade and purchased from Sinopharm Chemical Reagent (Shanghai, China). BSA was obtained from Sigma–Aldrich (St. Louis, MO, USA). Sequencing grade trypsin was from Promega (Madison, WI, USA). Thymidine, uridine, adenosine, cytidine and guanosine were purchased from Shanghai Kayon Biological Technology (Shanghai, China). The standard solutions of each analyte were prepared in methanol at 1 mg/mL and stored at 4 °C in dark.

2.2. Preparation of the monoliths

The polymer monolith was in situ prepared inside a fused silica capillary (100 μm *i.d.*), which was derivatized with 3-(triethoxysilyl) propyl methacrylate [41]. The poly(MAA-*co*-EDMA) monolith was prepared by one-step polymerization. Briefly, porogen PEG was dissolved in DMSO and thoroughly mixed to ensure that the solution was completely homogeneous. Subsequently, monomer MAA and crosslinker EDMA were added into the solution with the amounts listed in Table 1. The mixture was then briefly shaken before adding the initiator AIBN (1% (w/w) with respect to monomer) to the solution. The polymerization mixture was completely mixed by vortexing and ultrasonication to form a homogeneous solution and to remove oxygen. To remove inhibitors, monomer MAA and EDMA were extracted with 10% aqueous sodium hydroxide and water [42,43]. And we examined the effect of removal of the inhibitors on the properties and performance of monolithic columns. The resulting solution was then filled into the capillary to generate 10 cm and 30 cm monoliths for backpressure measurement and *c*LC experiment, respectively. Both ends of the capillary were sealed by silicon rubber for polymerization at 60 °C for 12 h. Finally, the monolithic capillary was washed with methanol under a pressure of 18 MPa for 5 h.

Meanwhile, monoliths with PEG of different molecular weight (Table 2) were prepared in centrifuge tubes for surface area and pore size distribution measurements. After polymerization, the monoliths were cut into small cubic pieces (approximate 1 mm^3) and submersed in hot (70 °C) water/methanol (1:1, v/v) for at least 4 h to remove the PEG and non-reacted chemicals [38]. The washing was repeated three times followed by drying in oven at 60 °C and the resulting samples were kept in dry vials before characterization.

To evaluate the influence of different porogens on the properties of monolith, poly(MAA-*co*-EDMA) monolithic columns were also prepared using toluene and dodecanol according to previous work [33,44].

2.3. Instrument and analytical conditions

The surface area and mesopore size distribution of poly(MAA-*co*-EDMA) monoliths were measured by nitrogen adsorption–desorption experiments with a JW-BK surface area and pore size analyzer from JWGB Sci & Tech (Beijing, China). Before measurement, the monolithic cubic pieces were evacuated in vacuum, and heated to 393 K for 3 h to remove the physically adsorbed substances. The macroporous properties of the monoliths were determined by mercury intrusion porosimetry (MIP) using an Autopore IV 9500 mercury porosimeter (Micromeritics, Norcross, USA) [45]. Surface area values were determined by the Brunauer–Emmett–Teller (BET) equation at P/P_0 between 0.05 and 0.2 [46]. Mesopore size distributions were evaluated from the desorption branches of isotherms based on the Barrett–Joyner–Halenda (BJH) model [47]. The microscopic morphology of the monoliths was examined by SEM using a QUANTA-200 instrument of FEI (Eindhoven, Netherlands). Prior to measurement, the monolithic capillary samples were cut into 2 mm long pieces, placed on an aluminum stub and then sputter-coated with gold.

Permeability measurements were performed using a Shimadzu (Kyoto, Japan) LC-10AT pump under constant flow mode. Methanol was pumped through the 10 cm-long capillaries at flow rate of 2 μL/min. The backpressure was recorded when the pressure stabilized.

Permeability (K, m^2) was calculated according to Darcy's Law by using the following equation [48,49]:

$$K = \frac{u\eta L}{\Delta P} \quad (1)$$

where u (m/s) is the linear velocity of mobile phase, η is the viscosity of mobile phase (0.60×10^{-3} Pa s at 20 °C with using methanol), L is the length of the monolithic column (m) and ΔP is the pressure drop across the monolithic column (Pa).

All *c*LC experiments were performed on a SHIMADZU *c*LC system containing one FVC nano valve with two position, a 50 nL sample loop, two Shimadzu LC-20A nano pumps (Tokyo, Japan) and one GL Sciences MU 701 UV–vis detector with a 6 nL

detection cell (Tokyo, Japan). After connecting to the *c*LC system, the poly(MAA-*co*-EDMA) monolith was conditioned with the mobile phase (ACN/H_2O (50/50, v/v)) at a low flow rate of 200 nL/min for 30 min. The chromatograms of benzoic acids were recorded at a wavelength of 214 nm, and other analytes were recorded at a wavelength of 254 nm.

To determine the cation-exchange capacities of the monolithic columns, the frontal analysis was performed according to previous method [30]. The measurement was carried out with poly(MAA-*co*-EDMA) monolith columns (100 μm *i.d.* × 30 cm) on SHIMADZU *c*LC system above. The detection wavelength was set at 258 nm and the flow rate was set at 400 nL/min. The ion-exchange capacities were calculated by Cu^{2+} (1 μmol/L) breakthrough measurements.

2.4. Tryptic digestion of BSA

BSA (1 mg) was dissolved in 100 μL of 100 mM Tris–HCl (pH 8.5) containing 8 M urea. The protein solution was mixed with 5 μL 100 mM tri(2-chloroethyl)phosphate and incubated for 20 min at room temperature to reduce protein disulfide bonds. 3 μL 500 mM Iodoacetamide was added to the solution and incubated for an additional 30 min at room temperature in dark. The reduced and alkylated protein mixture was diluted with 300 μL 100 mM Tris–HCl (pH 8.5) and then 9 μL 100 mM $CaCl_2$ was added to the above solution. The mixture (50 μL) was digested with trypsin at an enzyme to substrate ratio of 1:50 (w/w) by incubating at 37 °C for overnight.

2.5. cLC–MS/MS analysis of tryptic digests of BSA

The tryptic digests of BSA were separated on a Shimadzu nano-Prominence (*c*LC) system (Kyoto, Japan) coupled with a micrOTOFq orthogonal-accelerated time-of-flight mass spectrometer from Bruker Daltonics (Bremen, Germany), which was controlled by Bruker Daltonics Hystar. Bruker Daltonics Data analysis 3.4 software was employed for the data analysis. Transfer parameters were optimized by direct infusion of an ESI tuning mix from Agilent Technologies (Waldbronn, Germany). Spectra were collected with a time resolution of 1 s in the *m*/*z* range of 500–2500.

Under *c*HILIC mode, a 5 cm "hydrophilic" poly(MAA-*co*-EDMA) monolith was used as trap column. Tryptic digests of BSA were automatically injected into the trap column at a flow rate of 5 μL/min for 18 min with carrier solution of water/ACN (1/99, v/v), considering the loading tube volume was ~85 μL. The trapped peptides were then separated at a flow rate of 500 nL/min on a 30 cm "hydrophilic" monolithic column (100 μm *i.d.*), which was connected to a PicoTip™ (New Objective, Woburn, MA) nanospray tip (360 μm *o.d.*, and 10 μm *i.d.* spray tip) with a zero-dead volume union (Upchurch Scientific, Oak Harbor, WA, USA) to minimize post column dead volumes.

Under RP mode, a C_{18} column (2 cm × 100 μm *i.d.*, 5 μm) from Weltech (Wuhan, China) was used for online trap column. Tryptic digests of BSA were injected into the trap column with carrier solution of water/ACN/formic acid (99/1/0.1, v/v/v). A GL sciences Inertsil ODS-3 capillary EX-nano column (150 mm × 75 μm *i.d.*, 3 μm) was used as the analytical column at a flow rate of 200 nL/min. The rest analyzing conditions are the same as that under *c*HILIC mode.

The peptide identification was performed using an in-house version of Mascot v2.2 (Matrix Science, London, U.K.). The MS/MS data were searched against the SwissPort database. Peptide identifications were restricted to tryptic peptides with no more than two missed cleavages. The mass tolerances were 20 ppm for precursor ions and 0.1 Da for fragment ions. To evaluate the false discovery rate (FDR) of peptides identification, a decoy database created by Mascot was applied to the database search, and the FDR was controlled at <1% by setting the Mascot score ($p < 0.05$).

Table 3
Permeability (*K*) of the monoliths prepared with PEG of different molecular weight and amounts.[a]

	PEG M.W.	PEG (%, w/w_{total})	State of column	K ($\times 10^{-14}$ m^2)
Column 10	6000	9.1	Sol state	1.23
Column 11	6000	13.0	Sol state	6.83
Column 12	6000	16.7	Slack, slight detached	13.70
Column 13	6000	20.0	Homogeneous	19.80
Column 14	6000	23.1	Homogeneous	19.90
Column 15	4000	20.0	Slack, slight detached	1.19
Column 16	4000	27.3	Slack, slight detached	6.93
Column 17	4000	30.4	Homogeneous	18.40
Column 18	4000	33.3	Homogeneous	20.30

[a] The ratio of monomers (MAA and EDMA) and DMSO is 1/3 (w/w). The percent of MAA and EDMA ($w/w_{total\ monomers}$) is 8% and 92%, respectively.

3. Results and discussion

3.1. Preparation of the column

Since the separation process is performed under pressure, the monolith should possess high mechanical stability as well as satisfactory permeability. Additionally, a homogeneous monolith is desired to achieve high column efficiency. Therefore, several factors including porogen types, ratio of functional monomer to crosslinker, ratio of monomers to porogen were optimized to obtain good chromatographic performance.

3.1.1. Effect of monomer amount on porous structure

An alteration in monomer to crosslinker ratio can change the porosity, rigidity and homogeneity of the monolith [50]. To evaluate the effect of monomer amount on the porous structure of polymer monolith, the MAA in the polymerization mixture ranging from 5.00% to 12.5% ($w/w_{total\ monomers}$) were examined (Table 1). The results showed that the permeability increased with the elevated ratio of MAA to EDMA (Table 1, from column 1 to column 5). Normally large ion-exchange capacity can be achieved with the increased percentage of MAA, but the higher content of MAA will result in inhomogeneous column bed, therefore, 8% MAA ($w/w_{total\ monomers}$) was used for the preparation of the monolithic column.

3.1.2. Effect of PEG on porous structure

In order to obtain a monolithic column with homogeneous through-pore, appropriate permeability and large specific surface area, the effect of PEG with molecular weight ranging from 2000 to 10,000 on the polymerization was investigated. The results showed that with the increase of the molecular weight of PEG, the permeability increased but the specific surface area decreased (Table 2). Increase of the molecular weight of PEG resulted in a solvated system with higher steric hindrance, and therefore larger through-pore, which was consistent with previous report [37,38,41,51]. In this respect, PEG-6000 and PEG-4000 were selected for further optimization.

The effects of PEG amount on the porous structure of monolith were further studied (Table 3, column 10–18). The permeability of prepared monoliths increased with the increase of PEG amount (Table 3). Normally a separation monolith should possess appropriate permeability around 19×10^{-13} m^2 (approximate 8 MPa at 500 nL/min). Our results showed that four monoliths (column 13, 14, 17, 18) had permeability between 18.4×10^{-13} and 20×10^{-13} m^2. Therefore, the kinetic performance of these four monoliths was further examined (Fig. S1, SI).

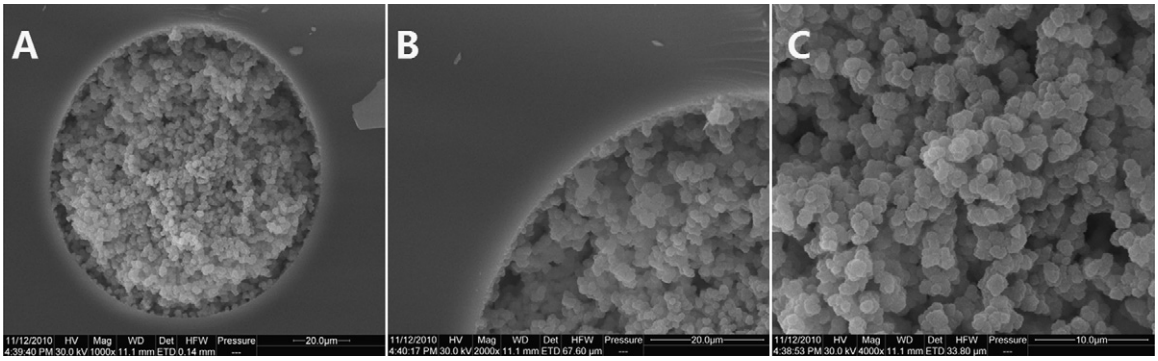

Fig. 1. Scanning electron microscope images of the cross section of the monolith prepared under optimized conditions (Table 3, column 13). (A) Wide-view; (B), (C) close-up-view.

The effects of various linear flow velocity (u) on plate height (H) could by described by the van Deemter equation

$$H = A + \frac{B}{u} + Cu \quad (2)$$

where the three parameters A, B, and C represented eddy dispersion, longitudinal diffusion, and mass transfer resistance, respectively. It suggested that column 13 had the highest column efficiency with 48,000 plates/m at a flow velocity of 0.43 mm/s for acrylamide, in which the plate height was approximate 20.8 μm (Fig. S1, SI).

Taken together, the optimized polymerization mixture consisted of 1.6% ($w/w_{total\ monomers}$) MAA, 18.4% ($w/w_{total\ monomers}$) EDMA, 60% ($w/w_{total\ monomers}$) DMSO and 20% ($w/w_{total\ monomers}$) PEG-6000.

3.1.3. Preparation of "hydrophobic" monolith

The "hydrophobic" monolithic column was also prepared by using dodecanol and toluene instead of PEG and DMSO for the polymerization. To obtain a continuous and homogeneous column bed, the ratio of MAA to EDMA was firstly optimized (Table S1, SI). The results showed that with the increase of MAA percentage from 20% to 50% ($w/w_{total\ monomers}$), the permeability increased; however, over 40% ($w/w_{total\ monomers}$) MAA can result in slack monoliths. Thus, 30% ($w/w_{total\ monomers}$) MAA was chosen for further experiments.

Then, the effect of the dodecanol amount on the porous structure of monolith was evaluated from 9.66% to 22.8% (w/w_{total}) (Table S2, SI). The results revealed that better permeability can be achieved with the increase of dodecanol. But too much dodecanol (22.8% (w/w_{total}) dodecanol, column S9) can cause the slack of the monolith. Column S7 and column S8 showed homogenous column bed and good permeability (19.5×10^{-13} and 20×10^{-13} m^2 for column S7 and column S8, respectively, Table S2, SI), therefore the kinetic performance of these two columns were further examined (Fig. S2, SI). It suggested that column S7 had the higher column efficiency with 29,000 plates/m for acrylamide at a flow velocity of 0.2 mm/s, in which the plate height was approximate 34.5 μm. Although column 13 (Table 3) and column S7 (Table S2, SI) had different composition of the monomers depending on the type of porogen, comparison of the kinetic performance between column 13 and column S7 was of interest considering both of them were at their own optimum.

With respect to the effect of porogens on retentive properties, the comparison at the same monomer composition would be of interest. To this end, the "hydrophobic" monolith was also prepared with using the same ratio of MAA to EDMA as that of the monolith prepared with PEG and DMSO. The results showed that the surface are of monolithic column decreased from 188 to 50 m^2/g with the increase of dodecanol amount (Table S3, SI). Considering that column S12 had both appropriate surface area and permeability, we chose it for further HILIC comparison experiments.

3.2. Characterization of the monolithic columns

The through-pores size distributions of monolithic columns were determined by mercury intrusion porosimeter analysis. The results showed that more narrow distribution of through-pores size with approximate 1 μm was observed on column 13, while column S7 had wide distribution of through-pores size ranging from 1 to 10 μm (Fig. S3, SI). And the column S12, which was made with the same ratio of MAA to EDMA as column 13, also showed wide distribution of through-pores size ranging from 1 to 12 μm (Fig. S3, SI). Normally narrow through-pores size distribution suggested homogeneous column bed and high column efficiency. In this respect, the results indicated that the porogen system of PEG and DMSO can generate narrower pore size distribution and more homogeneous column bed than the monolith prepared with dodecanol and toluene.

The morphology of the resulting poly(MAA-*co*-EDMA) monolithic columns was examined by SEM (Fig. 1). Cross section of the intact and homogeneous micro-globules can be clearly observed (Fig. 1A) and the monolith was well attached to the inner wall of the capillary (Fig. 1B). In addition, the micro-globules interconnected to form large clusters, which resulted in uniform polymer-based monolithic matrix with approximate 2 μm through-pores (Fig. 1C). The hydrophobic porogenic system, toluene and dodecanol, also can induce the formation of continuous column bed and large through-pores (Fig. S4, SI). However, the homogeneity of micro-globules in "hydrophobic" monolith is not as good as that in "hydrophilic" one, which was consistent with the result obtained from the comparison of the through-pore size distribution between "hydrophobic" column S7 and "hydrophilic" column 13 (Fig. S3, SI).

The column efficiency of the "hydrophilic" monolith was evaluated by changing the flow rate from 0.15 to 0.95 mm/s. The effect of the flow velocity (calculated from the retention time of toluene at different flow rate) on the plate height was examined by using acrylamide, thiourea and cytidine (Fig. 2). The results showed that the plate height first decreased when the linear velocity increased from 0.15 to 0.41 mm/s. This Van Deemter curves showed the lowest plate height was approximate 20.8 μm for acrylamide with a flow velocity of 0.43 mm/s (Fig. 2). Compared with the "hydrophobic" monolithic column (Table S2, SI, column S7), the column efficiency of "hydrophilic" monolithic column not only was much higher than that of "hydrophobic" one, but also decreased less significantly with the increase of flow rate (Fig. S5, SI).

The ion-exchange capacity of "hydrophilic" column (column 13, Table 3) and "hydrophobic" one (column S12, Table S3, SI) were 1.01 ± 0.43 μmol/g and 0.43 ± 0.22 μmol/g, respectively. Compared

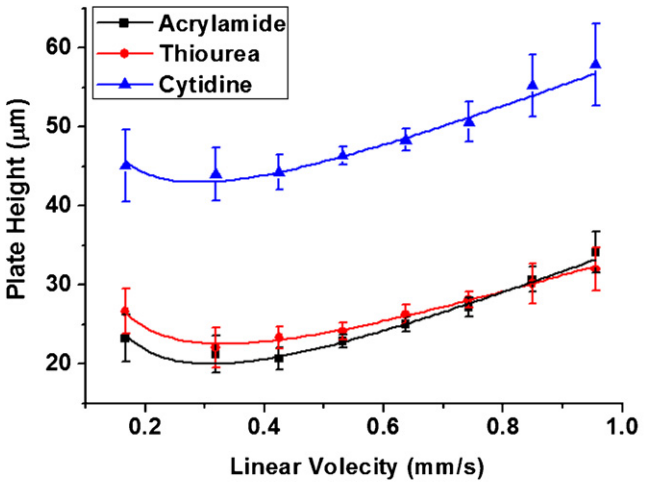

Van Deemter coefficients obtained after fitting the curves.

Column	A (μm)	B ($\times10^3\mu m^2s^{-1}$)	C ($\times10^{-3}$s)	H_{min} (μm)	$u_{optimal}$ (mm/s)
Cytidine	25.861	2.476	29.675	44.1	0.32
Thiourea	6.414	2.677	24.308	23.3	0.43
Acrylamide	1.132	2.920	30.424	20.8	0.43

Fig. 2. Van Deemter plot of the height equivalent to a theoretical plate as a function of flow rate. Experimental conditions: "hydrophilic" monolithic column, 100 μm *i.d.* × 30 cm; mobile phase: ACN/water (90/10, v/v); UV detection wavelength: 254 nm.

with "hydrophobic" column, the larger ion-exchange capacity of "hydrophilic" column can provide stronger hydrophilic interaction for polar compounds as well as more prominent electrostatic retention for charged compounds. In addition, column 14 (Table 3) prepared using higher percentage of PEG than the above "hydrophilic" column, possessed larger ion-exchange capacity (1.14 ± 0.44 μmol/g), which indicated that PEG can increase the number of carboxylic acid group on the surface of monolith. The same phenomena was also reported by Courtois et al. [38].

3.3. Separation of nucleosides

A mixture of nucleosides including thymidine, uridine, adenosine, cytidine and guanosine was used to investigate the chromatographic performance of the monolithic column for polar neutral compounds that are difficult to retain and separate by RPLC [2]. Our results showed that the five nucleosides can be well separated and the retention times increased with a slight increase of the ACN content from 86% to 92% in mobile phase. And the retention time of guanosine prolonged most significantly from 13 to 42 min (Fig. 3A).

In addition, the HILIC behavior of "hydrophobic" monolith was also investigated (column S12) using cytidine as the probe (Fig. 3B). With the increase of ACN content from 90% to 99% (v/v) in mobile phase, the retention factor (k) increased significantly (column 13 and column 14); on the contrary, the k value slightly increased for column S12, which indicated that the hydrophilic porogen may promote the exposure of carboxylic acid groups of MAA on the monolith surface and then lead to the large ion-exchange capacity. The result was also consistent with the measurement of ion-exchange capacity.

3.4. Separation of anilines

The poly(MAA-*co*-EDMA) monolith also offers weak electrostatic interaction with basic analytes. To demonstrate the selectivity of the poly(MAA-*co*-EDMA) monolith to basic analytes, five anilines (aniline; *p*-nitroaniline; *p*-phenylenediamine; *N*-methylaniline; *N*,*N*-dimethylaniline) were used for the evaluation.

Firstly, the pH value of mobile phase played an important role in the selectivity in HILIC by changing the ionization of analytes and the polarity of stationary phases. Fig. S6, SI showed the best separation was achieved at pH 5.0. At pH of 9.0, the ionization of *N*,*N*-dimethylaniline and *p*-phenylenediamine were suppressed (*p*-phenylenediamine, pK_b: 7.8; *N*,*N*-dimethylaniline, pK_b: 7.9) and the electrostatic interaction between the analytes and stationary phase was weak. Therefore, a shorter retention times of *N*,*N*-dimethylaniline and *p*-phenylenediamine with low resolution were observed. At pH of 7.0 and 5.0, all the anilines were positively charged (aniline, pK_b: 9.4; *p*-nitroaniline, pK_b: 13.0; *N*-methylaniline, pK_b: 9.2) and the stationary phase with carboxyl groups was negatively charged. Thus, the electrostatic mechanism largely contributed to the hydrophilic interaction between anilines and organic monolith and led to the baseline separation. When the pH value decreased to 3.0, the ionization of carboxyl groups was suppressed. The electrostatic interaction between anilines and the stationary phase was weak, which led to the shorter retention time and lower resolution.

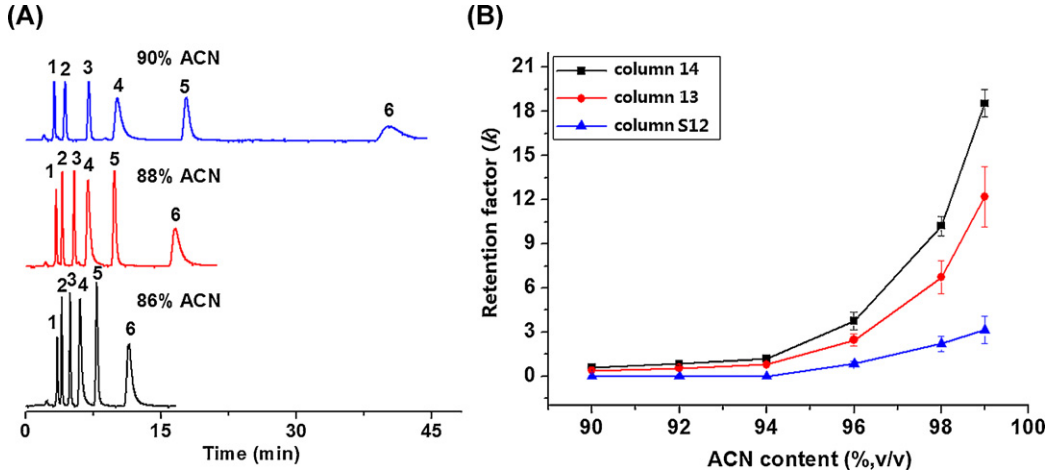

Fig. 3. (A) The effect of ACN content on the retention of nucleosides. Order of peaks: (1) toluene; (2) thymidine; (3) uridine; (4) adenosine; (5) cytidine; (6) guanosine. (B) The influence of ACN content on the retention of cytidine on different columns. Experimental conditions: monolithic capillary column, 100 μm *i.d.* × 30 cm; UV detection wavelength: 254 nm; flow rate: 500 nL/min; mobile phase: ACN/Water (v/v).

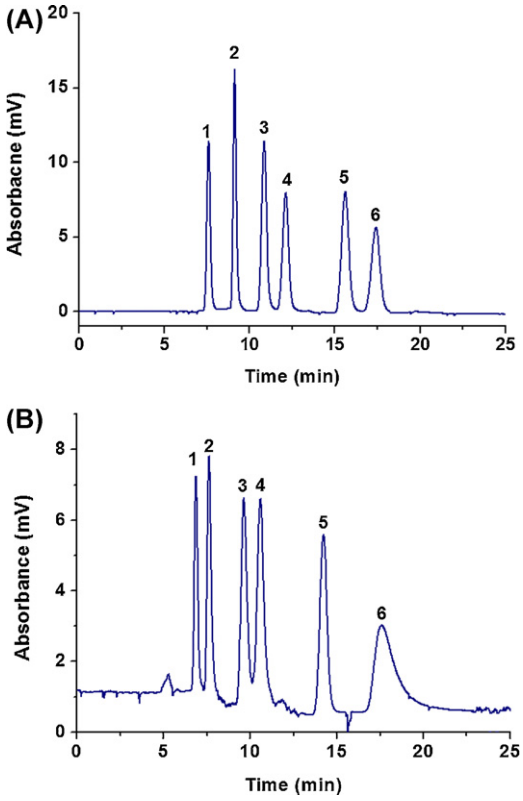

Fig. 4. (A) Chromatogram of anilines under optimized conditions. (B) Chromatogram of benzoic acids under optimized conditions. Experimental conditions: monolithic capillary column, 100 μm *i.d.* × 30 cm; UV detection at 254 nm for anilines, 214 nm for benzoic acids; flow rate: 400 nL/min; mobile phase for the separation of anilines: ACN/10 mM ammonium hydroxide (pH 5.0) (90/10, v/v); mobile phase for the separation of benzoic acids: ACN/50 mM ammonium formate (pH 4.0) (90/10, v/v). Order of peaks for (A): (1) toluene; (2) *p*-nitroaniline; (3) aniline; (4) *N*-methylaniline; (5) *p*-phenylenediamine; (6) *N*,*N*-dimethylaniline. Order of peaks for (B): (1) Toluene; (2) *p*-nitrobenzoic acid; (3) benzoic acid; (4) 3,5-dinitrobenzoic acid; (5) *p*-aminobenzoic acid; (6) *o*-aminobenzoic acid.

Additionally, the effect of salt concentration on the retention of five anilines was investigated by varying the concentration of ammonium formate (pH 5.0) from 0 to 30 mM in the mobile phase of ACN/water (90/10, v/v). As the ammonium formate concentration increased, the ion-exchange interactions weakened, which resulted in the shorter retention time of analytes. As a reflection, the value of retention factors ($\log k$) of five anilines linearly decreased with the increased ammonium formate concentration (Fig. S7, SI), which exhibited typical ion-exchange retention of anilines.

The content of ACN in the mobile phase had significant influence on the resolution and selectivity of anilines, and hydrophilic interactions were strengthened by increasing the ACN content. The value of retention factors ($\log k$) of five anilines increased linearly with the increase of ACN content in the mobile phase from 80% to 95% (v/v) (Fig. S8, SI). This result indicated that the separation of these analytes was conducted by the hydrophilic interaction between the analytes and the monolithic stationary phase. Fig. 4A showed the chromatogram of five anilines under optimized conditions and all of them were baseline separated within 20 min.

3.5. Separation of benzoic acids

Similar to the separation of anilines, the benzonic acids were also separated on poly(MAA-*co*-EDMA) monolith. At high pH value, the negatively charged molecules of benzoic acids had electrostatic repulsion with the carboxyl groups, which led to weak retention and low resolution of analytes. With the decrease of pH value, the amount of negatively charged molecules decreased and the electrostatic repulsion became weaker. Further decrease of the mobile phase pH suppressed the ionization of both analytes and the carboxyl groups on the monolithic column, which resulted in the weak retention of analytes. Finally, an effective separation of benzoic acids was obtained at mobile phase of pH 3.5.

Moreover, the retention factors ($\log k$) of benzoic acids decreased with the increased ammonium formate concentration from 10 mM to 40 mM, which could be attributed to a combined influence of the electrostatic repulsion. Weaker electrostatic repulsion led to stronger chromatographic retention, which caused longer migration time of analytes. The increased retention factors ($\log k$) with elevated ammonium formate concentration exhibited that the electrostatic repulsion influenced the separation of benzoic acids. Furthermore, the analytes retention increased with the increase of ACN content in the mobile phase, which clearly demonstrated that the monolithic column exhibited a typical HILIC chromatographic behavior towards acidic solutes. Fig. 4B showed the chromatogram of five benzoic acids under optimized conditions.

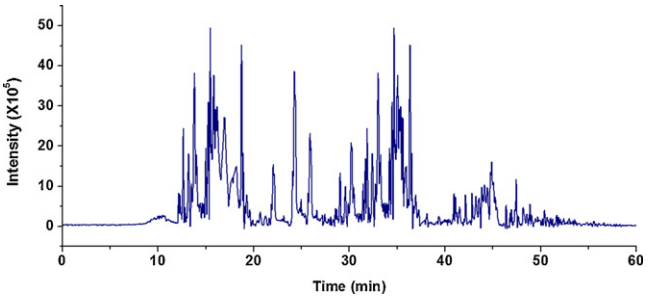

Fig. 5. Base peak chromatogram of tryptic digests of BSA with *c*HILIC-ESI-qTOF–MS analysis. Experimental conditions: 30 cm × 100 μm *i.d.* hydrophilic poly(MAA-*co*-EDMA) monolithic column. Mobile phase A: ACN containing 0.1% FA (v/v), mobile phase B: water containing 0.1% FA (v/v). Elution gradient: mobile phase B increased from 1% to 50% within 60 min at a flow rate 500 nL/min.

3.6. Separation of tryptic digests of BSA

Monolithic columns have hierarchical meso- and macro-porous structures, which lead to the fast mass transfer kinetics and lower backpressure during separation [52]. The unique property makes the monolithic columns, particularly silica-based monolithic columns [53,54], the emerging choice toward the conventional particulate-packed columns for the analysis of complex samples such as peptides and proteins. In this respect, with the hydrophilic polymer-based monolith, the HI separation of peptides mixture become an interesting choice in proteomics study [21,35].

The separation of peptides mixture derived from the tryptic digestion of BSA was performed on the prepared hydrophilic monolithic column using a *c*LC system coupled with ESI-qTOF-MS. 1 pmol of tryptic digests of BSA were loaded into the capillary monolithic column with a gradient elution by water from 1% to 50% (H_2O/ACN, v/v) within 60 min. Our results showed that 49 peptides were identified with 50.0% sequence coverage (RSD 4.2%, $n = 3$) (Table S4). Shown in Fig. 5 was the base peak chromatogram of the tryptic digests of BSA. In addition, the performance of "hydrophobic" monolith (column S7, Table S2) on the separation of the tryptic digests of BSA was also examined. However, only 25 peptides were identified with 36.0% sequence coverage was (RSD 7.8%, $n = 3$) (Table S5, Fig S9, SI).

Also, we performed the peptides mixture analysis using RPLC-ESI-qTOF–MS system, in which a particulate-packed commercial column (15 cm × 75 μm *i.d.*, 3 μm particles, GL Sciences) was used instead of the monolith. This results showed that 45 peptides

(RSD = 6.3%, $n = 3$) were identified with 40.0% sequence coverage (RSD = 5.1%, $n = 3$) (Table S6, Fig. S10, SI). Taken together, the results demonstrated that "hydrophilic" monolith provides a more powerful tool in the separation of complex samples.

3.7. Reproducibility

We assessed the effect of the removal of inhibitors on the properties and performance of monolithic column. After extraction with 10% aqueous sodium hydroxide and water, the permeability of monolith was 1.86×10^{-13} m^2 (RSD = 1.5%, $n = 3$) and the column efficiency for acrylamide was approximate 47,600 plates/m (RSD = 3.6%, $n = 3$). The retention time of 5 nucleosides (RSD = 0.8%, $n = 3$) was not apparently changed. The results showed that removal of inhibitors from the monomers and the removal of oxygen from the polymerization mixtures did not affect the properties of the columns. The run-to-run variation was evaluated on a single monolithic column for 5 runs, and the RSD for retention time of nucleosides on the "hydrophilic" monolithic column was 3.1% (Table S7). Both column-to-column and batch-to-batch variations for the "hydrophilic" monolithic columns were also evaluated with the RSDs of the retention time of nucleosides being 3.3% ($n = 5$) and 4.1% ($n = 3$), respectively (Table S7). In addition, the run-to-run, column-to-column and batch-to-batch variations for the "hydrophobic" monolithic column (column S7, Table S2) were examined with the RSDs of the retention time of nucleosides being 2.6%, 4.8%, and 9.1%, respectively (Table S7). And the retention time of analytes did not significantly change even after 50-time analysis. These results indicated that excellent reproducibility and reliable stability can be achieved using the capillary monolithic columns prepared in current study.

4. Conclusions

In current study, poly(MAA-*co*-EDMA) monolith has been successfully prepared for *c*HILIC using a hydrophilic porogenic system, PEG and DMSO. By optimizing the ratio of MAA to EDMA and the molecular weight and amount of PEG, the prepared monolithic column showed homogeneous and continuous column bed, good permeability and narrow pore size distribution. The column efficiency suggested a 48,000 plates/m using acrylamide. Under HILIC mode, five nucleosides were baseline separated on this monolithic column. Finally, this hydrophilic monolithic column was applied in the separation of tryptic digests of BSA with *c*HILIC-ESI-qTOF–MS system and 49 peptides were identified with 50.0% sequence coverage. Comparing to particulate-packed commercial column and the "hydrophobic" poly(MAA-co-EDMA) monolith prepared by toluene and dodecanol, the "hydrophilic" monolith prepared with PEG and DMSO shows much better chromatographic performance on the separation of complex samples. In this respect, "hydrophilic" monolith provides a promising approach for the proteomics study.

Acknowledgements

This work was supported by the National Science Fund for Distinguished Young Scholars (No. 20625516), the National Natural Science Foundation (No. 91017013; No. 31070327), the Science Fund for Creative Research Groups (No. 20921062), NSFC.

Appendix A. Supplementary data

Supplementary data associated with this article can be found, in the online version, at doi:10.1016/j.chroma.2012.01.065.

References

[1] A.J. Alpert, J. Chromatogr. 499 (1990) 177.
[2] Z.J. Jiang, N.W. Smith, P.D. Ferguson, M.R. Taylor, Anal. Chem. 79 (2007) 1243.
[3] F. Svec, J.M.J. Frechet, Anal. Chem. 64 (1992) 820.
[4] Z. Lü, P. Zhang, L. Jia, J. Chromatogr. A 1217 (2010) 4958.
[5] M.A. Jaoude, J. Randon, Anal. Bioanal. Chem. 400 (2011) 1241.
[6] Y. Li, H.D. Tolley, M.L. Lee, J. Chromatogr. A 1217 (2010) 8181.
[7] S. Karenga, Z. El Rassi, Electrophoresis 31 (2010) 3192.
[8] J. Lin, S.F. Liu, X.C. Lin, Z.H. Xie, J. Chromatogr. A 1218 (2011) 4671.
[9] X.C. Wang, K. Ding, C.M. Yang, X.C. Lin, H.X. Lu, X.P. Wu, Z.H. Xie, Electrophoresis 31 (2010) 2997.
[10] Z.J. Jiang, J. Reilly, B. Everatt, N.W. Smith, J. Chromatogr. A 1216 (2009) 2439.
[11] Z.J. Jiang, N.W. Smith, P.D. Ferguson, M.R. Taylor, J. Sep. Sci. 32 (2009) 2544.
[12] H.W. Zhong, Z. El Rassi, J. Sep. Sci. 32 (2009) 1642.
[13] T. Ikegami, K. Horie, N. Saad, K. Hosoya, O. Fiehn, N. Tanaka, Anal. Bioanal. Chem. 391 (2008) 2533.
[14] P. Jandera, J. Urban, V. Skerikova, P. Langmaier, R. Kubickova, J. Planeta, J. Chromatogr. A 1217 (2010) 22.
[15] J. Randon, S. Huguet, C. Demesmay, A. Berthod, J. Chromatogr. A 1217 (2010) 1496.
[16] J. Krenkova, N.A. Lacher, F. Svec, J. Chromatogr. A 1216 (2009) 3252.
[17] Y. Li, M.L. Lee, J. Sep. Sci. 32 (2009) 3369.
[18] D. Hoegger, R. Freitag, J. Chromatogr. A 1004 (2003) 195.
[19] S. Hjertén, J.-L. Liao, R. Zhang, J. Chromatogr. 473 (1989) 273.
[20] F. Svec, M. Petro, J.M.J. Frechet, Collect. Czech. Chem. Commun. 66 (2001) 1047.
[21] P. Hemstrom, A. Nordborg, K. Irgum, F. Svec, J.M.J. Frechet, J. Sep. Sci. 29 (2006) 25.
[22] E.F. Hilder, F. Svec, J.M.J. Frechet, Electrophoresis 23 (2002) 3934.
[23] J. Martens-Lobenhoffer, S. Postel, U. Tröger, S.M. Bode-Böger, J. Chromatogr. B 855 (2007) 271.
[24] Q. Ma, M. Chen, H.-R. Yin, Z.-G. Shi, Y.-Q. Feng, J. Chromatogr. A 1212 (2008) 61.
[25] T. Ikegami, K. Horie, J. Jaafar, K. Hosoya, N. Tanaka, J. Biochem. Biophys. Methods 70 (2007) 31.
[26] J. Wohlgemuth, M. Karas, T. Eichhorn, R. Hendriks, S. Andrecht, Anal. Biochem. 395 (2009) 178.
[27] V. Kumar, T. Yang, Y. Yang, Int. J. Pharm. 188 (1999) 221.
[28] M.H.J. Selman, L.A. McDonnell, M. Palmblad, L.R. Ruhaak, A.M. Deelder, M. Wuhrer, Anal. Chem. 82 (2010) 1073.
[29] J. Dong, J.J. Ou, X.L. Dong, R.N. Wu, M.L. Yel, H.F. Zou, J. Sep. Sci. 30 (2007) 2986.
[30] M.L. Chen, M.M. Zheng, Y.Q. Feng, J. Chromatogr. A 1217 (2010) 3547.
[31] N. Tan, G.Y. Xiao, D.Y. Yan, G.M. Sun, J. Membr. Sci. 353 (2010) 51.
[32] G.H. Huang, Q.Y. Lian, W.C. Zeng, Z.H. Xie, Electrophoresis 29 (2008) 3896.
[33] H.Y. Yan, L.M. Jin, K.H. Row, Korean J. Chem. Eng. 23 (2006) 625.
[34] M.-L. Chen, S.-S. Wei, B.-F. Yuan, Y.-Q. Feng, J. Chromatogr. A, doi:10.1016/j.chroma.2011.07.061, in press.
[35] X. Chen, H.D. Tolley, M.L. Lee, J. Sep. Sci. 34 (2011) 2088.
[36] E.C. Peters, F. Svec, J.M.J. Frechet, C. Viklund, K. Irgum, Macromolecules 32 (1999) 6377.
[37] A. Palm, M.V. Novotny, Anal. Chem. 69 (1997) 4499.
[38] J. Courtois, E. Bystrom, K. Irgum, Polymer 47 (2006) 2603.
[39] S. Saeki, N. Kuwahara, M. Nakata, M. Kaneko, Polymer 17 (1976) 685.
[40] Q. Ma, J. Xu, Y. Lu, Z.G. Shi, Y.Q. Feng, Anal. Methods 2 (2010) 1333.
[41] M. Chen, Y. Lu, Q. Ma, L. Guo, Y.Q. Feng, Analyst 134 (2009) 2158.
[42] P. Krajnc, N. Leber, D. Štefanec, S. Kontrec, A. Podgornik, J. Chromatogr. A 1065 (2005) 69.
[43] Y. Li, X. Xie, M.L. Lee, J. Chen, J. Chromatogr. A 1218 (2011) 8608.
[44] F. Wei, Y. Fan, M. Zhang, Y.-Q. Feng, Electrophoresis 26 (2005) 3141.
[45] Q.-W. Yu, X. Wang, Q. Ma, B.-F. Yuan, H.-B. He, Y.-Q. Feng, Anal. Methods, doi:10.1039/C1AY05412K, in press.
[46] S. Brunauer, P.H. Emmett, E. Teller, J. Am. Chem. Soc. 60 (1938) 309.
[47] E.P. Barrett, L.G. Joyner, P.P. Halenda, J. Am. Chem. Soc. 73 (1951) 373.
[48] K.F. Du, D. Yang, Y. Sun, J. Chromatogr. A 1163 (2007) 212.
[49] C. Martin, J. Coyne, G. Carta, J. Chromatogr. A 1069 (2005) 43.
[50] J. Lin, G.H. Huang, X.C. Lin, Z.H. Xie, Electrophoresis 29 (2008) 4055.
[51] Q. Ma, M. Chen, Z.-G. Shi, Y.-Q. Feng, J. Sep. Sci. 32 (2009) 2592.
[52] T. Yoshida, J. Biochem. Biophys. Methods 60 (2004) 265.
[53] J.-T. Wu, P. Huang, M.X. Li, D.M. Lubman, Anal. Chem. 69 (1997) 2908.
[54] M.H. Wu, R.A. Wu, F.J. Wang, L.B. Ren, J. Dong, Z. Liu, H.F. Zou, Anal. Chem. 81 (2009) 3529.